Spatiotemporal Patterns of Precipitation Use Efficiency of Grassland Vegetation in Northwestern China Postprint

Authors: Mu Shaojie, You Yongliang, Zhu Chao, Zhou Kexin

Date: 2017-03-22T00:00:00+00:00

Abstract

Vegetation precipitation use efficiency (PUE) is an important indicator for evaluating the response characteristics of vegetation productivity to spatiotemporal dynamics of precipitation in arid and semi-arid regions. The net primary productivity (NPP) of grassland vegetation in seven northwestern provinces of China from 2001 to 2010 was estimated using the light use efficiency CASA (Carnegie-Ames-Stanford Approach) model. Combined with spatial interpolation data of precipitation, we analyzed the spatial distribution of grassland vegetation PUE, PUE of major vegetation types, and the driving factors of their spatiotemporal patterns. The results showed that: (1) The average PUE of grassland vegetation in the seven northwestern provinces from 2001 to 2010 was 0.68 g C m-2mm-1. Among various temperate grassland types, the order of PUE was meadow steppe > shrubland > typical steppe > desert steppe > desert, with significant differences in PUE among different grassland types; for alpine grasslands, the PUE of alpine steppe was significantly higher than that of alpine meadow; (2) The relationship between the spatial distribution of temperate grassland PUE and annual precipitation followed a parabolic shape (R2=0.65, P<0.001), with the PUE peak occurring in areas with annual precipitation P=472.9 mm; the relationship between the spatial distribution of vegetation PUE in desert areas and annual precipitation also followed a parabolic shape (R2=0.63, P<0.001), with the PUE peak occurring in areas with annual precipitation P=263.2 mm; for alpine grasslands, vegetation PUE showed large variation in areas with annual precipitation below 100 mm, while in areas with annual precipitation greater than 100 mm, the spatial distribution of vegetation PUE with precipitation change followed a parabolic shape (R2=0.47, P<0.001), with the PUE peak occurring at P=559.2 mm; (3) In different precipitation zones, the relationship between interannual fluctuations of vegetation PUE and climate factors also varied considerably. In areas with annual precipitation of 200-1000 mm, the interannual fluctuations of grassland PUE were positively correlated with changes

in annual precipitation; in areas with annual precipitation higher than 1050 mm, the interannual fluctuations of grassland PUE showed a strong correlation with mean annual temperature, with correlation coefficients reaching up to 0.4.

Full Text

Preamble

ACTA ECOLOGICA SINICA ChinaXiv Partner Journal Vol. 37, No. 5 Mar., 2017 DOI: 10.5846/stxb201509281977

Spatio-temporal Patterns of Precipitation-Use Efficiency of Grassland in Northwestern China, 2017, 37(5): 1458-1471.

MU Shaojie[1], YOU Yongliang[2], ZHU Chao[1], ZHOU Kexin[1]

[1]Nanjing Institute of Environmental Sciences, Ministry of Environmental Protection, Nanjing 210042, China
[2]Dry Farming Institute, Hebei Academy of Agricultural and Forestry Sciences, Hengshui 053000, China

Corresponding author. E-mail: zkx@nies.org

Abstract

Precipitation-use efficiency (PUE) is a critical indicator for evaluating how vegetation productivity responds to spatio-temporal dynamics of precipitation in arid and semi-arid regions. Using the light-use efficiency CASA (Carnegie-Ames-Stanford Approach) model, this study estimated net primary productivity (NPP) of grassland vegetation in seven northwestern provinces of China from 2001-2010 based on MOD13A1 data and spatially interpolated meteorological data. PUE was calculated as the ratio of NPP to annual precipitation. The results showed that: (1) The multi-year average PUE of grassland in Northwestern China was 0.68 g C m^{2} mm^{1}. Among temperate grassland types, meadow steppe exhibited the highest PUE, while desert grassland showed the lowest, with significant differences between grassland types. For alpine grassland, alpine steppe had significantly higher PUE than alpine meadow. (2) Spatially, temperate grassland PUE increased initially, peaking at approximately 472.9 mm/a, then decreased along the precipitation gradient ($R^2 = 0.65$, $P < 0.001$). Desert PUE showed a similar parabolic relationship with precipitation ($R^2 = 0.63$, $P < 0.001$), with maximum PUE occurring at 263.2 mm annual precipitation. For alpine meadow, PUE was low at both dry (<100 mm) and wet ends of the precipitation gradient, peaking around 559.2 mm ($R^2 = 0.47$, $P < 0.001$). (3) Temporally, inter-annual PUE variation responded differently to climatic factors across precipitation ranges. In areas with 200-1000 mm precipitation, PUE was positively correlated with precipitation. In regions receiving >1050 mm precipitation, temperature had much greater effects than precipitation on inter-annual PUE variations.

Keywords: precipitation-use efficiency (PUE); fraction of vegetation cover (FVC); temperate grassland; alpine grassland; conceptual model

Introduction

For terrestrial ecosystems, precipitation is typically the key factor controlling ecosystem structure and functional dynamics, influencing biodiversity. This is particularly evident in arid and semi-arid regions, which account for a large proportion of land area. Previous studies on ecosystems worldwide have shown that vegetation net primary productivity (NPP) is positively correlated with annual precipitation. Precipitation-use efficiency (PUE), defined as the ratio of vegetation NPP to annual precipitation, reflects the relationship between photosynthetic assimilation processes and water consumption characteristics. It represents vegetation' s capacity to convert nutrients into biomass using water and serves as an important indicator for analyzing and evaluating vegetation productivity responses to precipitation spatio-temporal variations at regional scales. Studying vegetation PUE patterns along meteorological factor gradients helps further understand climate change impacts on ecosystems.

Research on NPP variation along precipitation gradients has focused on two aspects: spatial differences in multi-year average NPP among different regions along precipitation gradients, and temporal differences in NPP fluctuations within the same region across years. Due to variations in temporal and spatial scales among studies, conclusions have been inconsistent. Le Houérou et al. suggested that spatially, as aridity and potential evapotranspiration increase, precipitation variability and the percentage of ineffective precipitation increase, leading to decreasing PUE trends. Paruelo et al., based on 12 biomes, found that PUE tends toward a common peak in the driest years. Huxman et al., studying 14 biomes, concluded that PUE tends toward a common peak in the driest years and a common trough in the wettest years. Bai et al., examining a 4500 km grassland transect in Inner Mongolia, found PUE first increased then decreased with precipitation, peaking at 400–600 mm. These studies, mostly based on narrow precipitation intervals, yielded different conclusions.

Grassland is China' s most widely distributed terrestrial ecosystem, covering about 40% of the country's land area. As an important agricultural and pastoral production base with intense human activity, most grassland vegetation occurs in arid and semi-arid regions with fragile ecological environments, making it highly sensitive to global climate change. Precipitation is the primary limiting factor for grassland ecosystem functions, largely determining ecosystem function and variability. Previous studies on western China' s grasslands were mostly based on measured data from limited field sites, restricting temporal and spatial scales and yielding varying results. The representativeness of selected sites also affected conclusions. The widespread application of remote sensing data and ecological models provides effective means to explore long-term PUE spatio-temporal patterns at larger scales, reflecting vegetation conditions at pixel scales more comprehensively.

This study combines remote sensing imagery and meteorological data to investigate vegetation PUE spatio-temporal patterns and climate impacts in northwestern China using the CASA model. This will enhance understanding of vegetation productivity formation processes in arid and semi-arid regions and provide basis for assessing global climate change impacts on ecosystem carbon and water cycles.

1. Methods

1.1 PUE Calculation Methods

Different studies employ varying PUE calculation methods depending on research objectives and data availability. In ground-based studies, researchers typically use aboveground net primary productivity (ANPP) to calculate PUE = ANPP/PPT, assuming a fixed ratio between ANPP and NPP in arid ecosystems. When using remote sensing data, annual NPP is often simulated to calculate PUE = NPP/PPT. Since NPP and normalized difference vegetation index (NDVI) show significant linear correlation, NDVI can be used to extract vegetation cover information.

1.2 CASA Model

The CASA model is a light-use efficiency model driven by remote sensing, vegetation, and soil data. It estimates vegetation NPP by calculating absorbed photosynthetically active radiation (APAR) from vegetation indices and combining it with light-use efficiency. The estimation formula is:

NPP(x, t) = APAR(x, t) × (x, t)

where APAR(x, t) represents APAR absorbed by pixel x in month t, and (x, t) represents actual light-use efficiency.

APAR depends on total solar radiation and vegetation absorption proportion:

APAR(x, t) = SOL(x, t) × FPAR(x, t) × 0.5

where SOL(x, t) is total solar radiation (MJ/m^2) and FPAR(x, t) is the fraction of PAR absorbed by vegetation.

Light-use efficiency refers to vegetation' s efficiency in converting APAR to organic carbon:

(x, t) = T (x, t) × T (x, t) × W (x, t) × *

where T and T represent temperature effects, W represents water stress, and * is maximum light-use efficiency.

The maximum light-use efficiency * varies significantly by vegetation type. Zhu et al. optimized * values for Chinese vegetation types using NPP data, which have been widely applied. This study adopts these values: evergreen needleleaf forest (0.389 g C/MJ), deciduous broadleaf forest (0.692 g C/MJ), evergreen

broadleaf forest (0.985 g C/MJ), needle-broad mixed forest (0.768 g C/MJ), shrubland (0.429 g C/MJ), grassland (0.542 g C/MJ), and cropland (0.475 g C/MJ).

1.3 Vegetation Cover Fraction Calculation

Vegetation cover fraction (FVC) is calculated using the pixel dichotomy model, assuming each pixel' s NDVI comprises vegetation and soil components:

NDVI = NDVI × FVC + NDVI × (1 - FVC)

where NDVI and NDVI represent NDVI for full vegetation cover and bare soil, respectively. FVC is calculated as:

FVC = (NDVI - NDVI) / (NDVI - NDVI)

In practice, maximum and minimum NDVI values during the growing season substitute for NDVI and NDVI :

FVC = (NDVI - NDVI) / (NDVI - NDVI)

1.4 Data Acquisition and Preprocessing

Remote Sensing Data: MOD13A1 NDVI data from NASA' s EOS/MODIS (2001–2010) with 16-day temporal resolution and 500 m spatial resolution. Data were processed using MRT tools for format conversion and reprojection to WGS84/Albers Equal Area Conic projection. Maximum value compositing (MVC) generated monthly NDVI images.

Meteorological Data: Monthly temperature and precipitation from 756 standard meteorological stations (China Meteorological Data Sharing Service Network). Kriging interpolation in ArcGIS generated raster datasets matching MODIS resolution and projection.

Land Cover Data: 1:100,000 land cover data from the Earth System Science Data Sharing Platform, based on 2000 Landsat TM/ETM imagery with 250 m resolution. Data include 6 primary and 25 secondary types. Grasslands were reclassified into meadow steppe, typical steppe, desert steppe, alpine meadow, alpine steppe, shrubland, and desert vegetation.

1.5 Model Validation

Validating regional NPP simulations is challenging. This study used aboveground biomass data from 63 Inner Mongolia grassland sites (August 2003–2005). Biomass was converted to NPP using a 1:5.73 aboveground:belowground ratio and 0.475 carbon conversion factor. Correlation analysis between simulated and observed NPP yielded $R^2 = 0.61$ ($P < 0.001$, $n = 63$), confirming CASA model suitability for northwestern China grasslands.

2. Results

2.1 Spatial Patterns of PUE in Northwestern China

The study region spans semi-humid, semi-arid, and arid zones with complex topography, creating distinct spatial heterogeneity in climate. Annual precipitation decreases from southeast to northwest, ranging from 600–800 mm in southern Tibet and western Sichuan Plateau to <100 mm in the Tarim Basin. Mean annual temperature shows latitudinal and altitudinal patterns, with colder temperatures (-4 to 0°C) on the Tibetan Plateau and Inner Mongolia' s Hulunbuir Plateau, and warmer temperatures (12–15°C) in the Tarim and Turpan Basins.

From 2001–2010, mean grassland PUE in northwestern China was 0.68 g C m ^{2} mm ^{1}. Spatial distribution was fragmented: highest values (1.5–3 g C m ^{2} mm ^{1}) occurred in the Altai Mountains (Xinjiang), Gannan Autonomous Prefecture, eastern Qilian Mountains, and central Yinshan Mountains; moderate values (0.5–1.5 g C m ^{2} mm ^{1}) in Hulunbuir and Xilingol Leagues; and lowest values (<0.5 g C m ^{2} mm ^{1}) in the Daxing' anling forest region, Qinghai-Tibet-Sichuan border area, and Alxa League.

2.2 PUE Distribution Among Grassland Types

Multi-year average PUE varied significantly among grassland types: meadow steppe (1.59 g C m ^{2} mm ^{1}) > typical steppe (1.24 g C m ^{2} mm ^{1}) > shrubland (0.97 g C m ^{2} mm ^{1}) > desert steppe (0.84 g C m ^{2} mm ^{1}) > alpine steppe (0.65 g C m ^{2} mm ^{1}) > alpine meadow (0.58 g C m ^{2} mm ^{1}) > desert vegetation (0.46 g C m ^{2} mm ^{1}). Temperate grassland PUE (0.96 g C m ^{2} mm ^{1}) significantly exceeded alpine grassland PUE (0.65 g C m ^{2} mm ^{1}).

2.3 PUE Spatial Variation Along Precipitation Gradients

Temperate Grassland: Mean annual precipitation was 271.5 mm (76.3% of area received 100–500 mm). PUE showed a parabolic relationship with precipitation, peaking at P = 472.9 mm (R^2 = 0.65, P < 0.001). In areas with 150–472.9 mm precipitation, PUE increased significantly with precipitation (R^2 = 0.57, P < 0.001). Both precipitation and temperature significantly influenced PUE spatial variation (PUE = -0.425 + 0.00557×P + 0.00368×T, R^2 = 0.49, P < 0.005), with precipitation contributing 1.5 times more than temperature.

Desert Vegetation: Mean precipitation was 154.2 mm (81.2% of area <200 mm). PUE also showed a parabolic relationship, peaking at P = 263.2 mm (R^2 = 0.63, P < 0.001). Below 100 mm, PUE decreased with increasing precipitation (PUE = 0.689 - 0.00141×P, R^2 = 0.25, P < 0.05). Precipitation and temperature explained 63% of PUE variation (PUE = 0.689 - 0.00141×P - 0.0146×T, R^2 = 0.63, P < 0.001), with stronger negative temperature effects.

Alpine Grassland: Mean precipitation was 366.1 mm (64.5% of area 200–525 mm). PUE showed a parabolic relationship, peaking at P = 559.2 mm (R^2

= 0.47, P < 0.001). In 200–525 mm zones, PUE increased significantly with precipitation (R^2 = 0.61, P < 0.001). Precipitation and temperature explained 75.3% of variation (PUE = -0.423 + 0.00516×P + 0.00457×T, R^2 = 0.753, P < 0.001), with precipitation and temperature effects being comparable.

2.4 Temporal Variation of PUE and Climate Factors

Inter-annual PUE variation (2001–2010) differed among grassland types: temperate grassland PUE fluctuated 0.36–0.55 g C m ^{2} mm ^{1} (±22.5% from mean), desert grassland 0.57–0.76 g C m ^{2} mm ^{1} (±21.2%), and alpine grassland 0.97–1.22 g C m ^{2} mm ^{1} (±14.9%).

Spatial correlation patterns revealed: PUE-precipitation correlations ranged widely (-0.7 to 0.7), with strongest positive correlations (0.45–0.6) on the Tibetan Plateau, southeastern Qinghai, and western Sichuan Plateau. Negative correlations (-0.3) occurred in the Tarim Basin, Qaidam Basin, and western Alxa League. PUE-temperature correlations were weaker (-0.2 to 0.2), with moderate positive correlations (0.4–0.6) in southeastern Tibetan Plateau, western Sichuan, and northern Xinjiang.

2.5 PUE-Climate Relationships Along Precipitation Gradients

PUE-precipitation correlation varied parabolically with precipitation: negative in <200 mm zones, increasingly positive in 200–1000 mm zones (peaking at 1000 mm), then declining in >1000 mm zones. PUE-temperature correlation remained weakly positive (0–0.2) across most precipitation ranges but strengthened (up to 0.6) in >1050 mm zones, where low temperatures become the primary growth-limiting factor.

3. Discussion

3.1 PUE Distribution Range

The 2001–2010 PUE range (0.42–1.59 g C m ^{2} mm ^{1}) aligns with global arid grassland estimates (0.24–0.71 g C m ^{2} mm ^{1}) and Inner Mongolia grassland results (0.13–0.64 g C m ^{2} mm ^{1}). Temperate grassland PUE (0.96 g C m ^{2} mm ^{1}) exceeded alpine grassland PUE (0.65 g C m ^{2} mm ^{1}), possibly due to harsh alpine conditions (short growing season, intense solar radiation) limiting water-use efficiency.

3.2 PUE Spatial Patterns Along Precipitation Gradients

The parabolic PUE-precipitation relationship, peaking at 472.9 mm (temperate), 263.2 mm (desert), and 559.2 mm (alpine), reflects trade-offs between water limitation and nutrient leaching. In dry regions, water is the primary growth-limiting factor, so PUE increases with precipitation. In wet regions, saturated soils limit root oxygen availability, reduce microbial activity, and cause nutrient leaching, decreasing PUE.

The lower precipitation optimum for desert vegetation (263.2 mm) reflects adaptations: high root:shoot ratios, small leaf area, and low stomatal conductance limit responses to precipitation increases. Exceptionally high PUE in extremely arid areas (<100 mm) may result from: (1) topographic redistribution (e.g., alpine snowmelt feeding desert margins), (2) deep root systems accessing subsurface water, and (3) xerophytic species (e.g., *Haloxylon ammodendron*, *Calligortum mongolicum*) with high water-use efficiency.

3.3 PUE Temporal Variation and Driving Factors

Inter-annual PUE variation correlates positively with precipitation in 200–1000 mm zones, consistent with previous studies. The parabolic correlation pattern reflects trade-offs between plant physiological traits (dominant in dry zones) and biogeochemical constraints (dominant in wet zones). In dry ecosystems, high root:shoot ratios and low relative growth rates reduce PUE sensitivity to precipitation changes. In wet ecosystems, high meristem density and rapid physiological adjustment increase sensitivity.

The strengthening PUE-temperature correlation in >1050 mm zones confirms temperature as the primary limiting factor in humid, cold regions like the Tibetan Plateau. The weakening PUE-precipitation correlation in extreme wet conditions reflects nutrient limitation and oxygen stress.

3.4 Conceptual Model

A conceptual model illustrates the trade-off between plant traits and biogeochemical factors along precipitation gradients. PUE spatial distribution peaks at intermediate precipitation where water and nutrient limitations are balanced. Inter-annual PUE variation is most sensitive to precipitation changes in these intermediate zones, while being constrained by physiological traits in dry zones and nutrient cycling in wet zones.

4. Conclusion

Based on remote sensing and meteorological data (2001–2010), this study reveals:

1. **Mean PUE** of northwestern China grasslands was 0.68 g C m^{-2} mm^{-1}, with fragmented spatial distribution. Among temperate grasslands, meadow steppe > typical steppe > desert steppe. Alpine steppe PUE significantly exceeded alpine meadow PUE.
2. **Spatial patterns:** Temperate and desert grassland PUE showed parabolic relationships with precipitation, peaking at 472.9 mm and 263.2 mm respectively. Alpine grassland PUE also showed a parabolic relationship, peaking at 559.2 mm.

3. **Temporal patterns:** Inter-annual PUE variation correlated positively with precipitation in 200–1000 mm zones. In >1050 mm zones, temperature effects exceeded precipitation effects.

4. **Mechanisms:** PUE-precipitation correlation strength varied parabolically with precipitation, being weakest at precipitation extremes due to physiological and biogeochemical constraints, and strongest at intermediate precipitation levels where vegetation is most sensitive to water availability changes.

These findings improve understanding of grassland ecosystem responses to climate change and provide scientific basis for regional carbon and water cycle management.

References

[1] Le Houérou HN, Bingham RL, Skerbek W. Relationship between the variability of primary production and the variability of annual precipitation in world arid lands. *Journal of Arid Environments*, 1988, 15(1): 1-18.

[2] Knapp AK, Smith MD. Variation among biomes in temporal dynamics of aboveground primary production. *Science*, 2001, 291(5503): 481-484.

[3] Bai YF, Wu JG, Qi X, Pan QM, Huang JH, Yang DL, Han XG. Primary production and rain use efficiency across a precipitation gradient on the Mongolia Plateau. *Ecology*, 2008, 89(8): 2140-2153.

[4] Sala OE, Parton WJ, Joyce LA, Lauenroth WK. Primary production of the central grassland region of the United States. *Ecology*, 1988, 69(1): 40-45.

[5] McNaughton SJ, Oesterheld M, Frank DA, Williams KJ. Ecosystem-level patterns of primary productivity and herbivory in terrestrial habitats. *Nature*, 1989, 341(6238): 142-144.

[6] Huxman TE, Smith MD, Fay PA, Knapp AK, Shaw MR, Loik ME, Smith SD, Tissue DT, Zak JC, Weltzin JF, Pockman WT, Sala OE, Haddad BM, Harte J, Koch GW, Schwinning S, Small EE, Williams DG. Convergence across biomes to a common rain-use efficiency. *Nature*, 2004, 429(6992): 651-654.

[7] Paruelo JM, Lauenroth WK, Burke IC, Sala OE. Grassland precipitation-use efficiency varies across a resource gradient. *Ecosystems*, 1999, 2(1): 64-68.

[8] Le Houérou HN. Rain use efficiency: a unifying concept in arid-land ecology. *Journal of Arid Environments*, 1984, 7(3): 213-247.

[9] [Reference text in Chinese - retained as in original]

[10] Hu ZM, Yu GR, Fan JW, Zhong HP, Wang SQ, Li SG. Precipitation-use efficiency along a 4500-km grassland transect. *Global Ecology and Biogeography*, 2010, 19(6): 842-851.

[11] Prince SD, De Colstoun EB, Kravitz LL. Evidence from rain-use efficiencies does not indicate extensive Sahelian desertification. *Global Change Biology*, 1998, 4(4): 359–374.

[12] [Reference text in Chinese - retained as in original]

[13] Lauenroth WK, Burke IC, Paruelo JM. Patterns of production and precipitation-use efficiency of winter wheat and native grasslands in the Central Great Plains of the United States. *Ecosystems*, 2000, 3(4): 344–351.

[14] Yan LM, Luo YQ, Sherry RA, Bell JE, Zhou XH, Xia JY. Rain use efficiency as affected by climate warming and biofuel harvest: results from a 12-year field experiment. *Global Change Biology Bioenergy*, 2014, 6(5): 556–565.

[15] [Reference text in Chinese - retained as in original]

[16] Yang YH, Fang JY, Fay PA, Bell JE, Ji CJ. Rain use efficiency across a precipitation gradient on the Tibetan Plateau. *Geophysical Research Letters*, 2010, 37(15): 78–82.

[17] Li H, Zhang FW, Li YN, Zhao X, Cao G. Thirty-year variations of above-ground net primary production and precipitation-use efficiency of an alpine meadow in the north-eastern Qinghai-Tibetan plateau. *Grass and Forage Science*, 2015, doi: 10.1111/gfs.12165.

[18] Lo Seen D, Mougin E, Rambal S, Gaston A, Hiernaux P. A regional Sahelian grassland model to be coupled with multispectral satellite data. II: Toward the control of its simulations by remotely sensed indices. *Remote Sensing of Environment*, 1995, 52(3): 194–206.

[19] Prince SD, Wessels KJ, Tucker CJ, Nicholson SE. Desertification in the Sahel: a reinterpretation of a reinterpretation. *Global Change Biology*, 2007, 13(7): 1308–1313.

[20] [Reference text in Chinese - retained as in original]

[21] Long HL, et al. [Reference text in Chinese - retained as in original]

[22] Ma WH, et al. [Reference text in Chinese - retained as in original]

[23] [Reference text in Chinese - retained as in original]

[24] [Reference text in Chinese - retained as in original]

[25] [Reference text in Chinese - retained as in original]

[26] [Reference text in Chinese - retained as in original]

[27] [Reference text in Chinese - retained as in original]

[28] Lauenroth WK, Sala OE. Long-term forage production of North American shortgrass steppe. *Ecological Applications*, 1992, 2(4): 397–403.

[29] Leith H. Modeling the primary productivity of the world // Leith H, Whittaker RH, eds. *Primary Productivity of the Biosphere*. Berlin Heidelberg: Springer, 1975: 237–263.

[30] Halse SA, Scanlon MD, Cocking JS, Smith MJ, Kay WR. Factors affecting river health and its assessment over broad geographic ranges: the Western Australian experience. *Environmental Monitoring and Assessment*, 2007, 134(1): 161–175.

[31] Austin AT, Vitousek PM. Nutrient dynamics on a precipitation gradient in Hawaii. *Oecologia*, 1998, 113(4): 519–529.

[32] Keddy PA. A pragmatic approach to functional ecology. *Functional Ecology*, 1992, 6(6): 621–626.

[33] Tilman D. *Plant Strategies and the Dynamics and Structure of Plant Communities*. Princeton: Princeton University Press, 1988.

[34] Wu XC, Liu HY, Ren J, He SY, Zhang YK. Water-dominated vegetation activity across biomes in mid-latitudinal eastern China. *Geophysical Research Letters*, 2009, 36(4): L04402, doi: 10.1029/2008GL036940.

[35] [Reference text in Chinese - retained as in original]

[36] Jobbágy EG, Sala OE. Controls of grass and shrub aboveground production in the Patagonian Steppe. *Ecological Applications*, 2000, 10(2): 541–549.

[37] [Reference text in Chinese - retained as in original]

[38] [Reference text in Chinese - retained as in original]

[39] Ehleringer JR, Cerling TE, Helliker BR. C4 photosynthesis, atmospheric CO2, and climate. *Oecologia*, 1997, 112(3): 285–299.

[40] Farquhar GD, O' Leary MH, Berry JA. On the relationship between carbon isotope discrimination and the intercellular carbon dioxide concentration in leaves. *Australian Journal of Plant Physiology*, 1982, 9(2): 121–137.

[41] Gutman G, Ignatov A. The derivation of the green vegetation fraction from NOAA/AVHRR data for use in numerical weather prediction models. *International Journal of Remote Sensing*, 1998, 19(8): 1533–1543.

[42] Lauenroth WK, Sala OE, Coffin DP, Kirchner TB. The importance of soil water in the recruitment of *Bouteloua gracilis* in the shortgrass steppe. *Ecological Applications*, 1994, 4(4): 741–749.

[43] Vinton MA, Burke IC. Interactions between individual plant species and soil nutrient status in shortgrass steppe. *Ecology*, 1995, 76(4): 1116–1133.

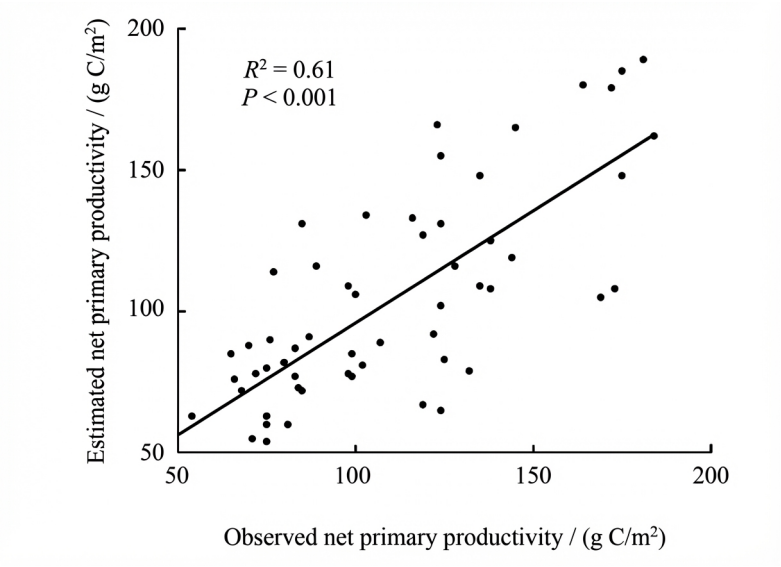

Figure 1: Figure 1

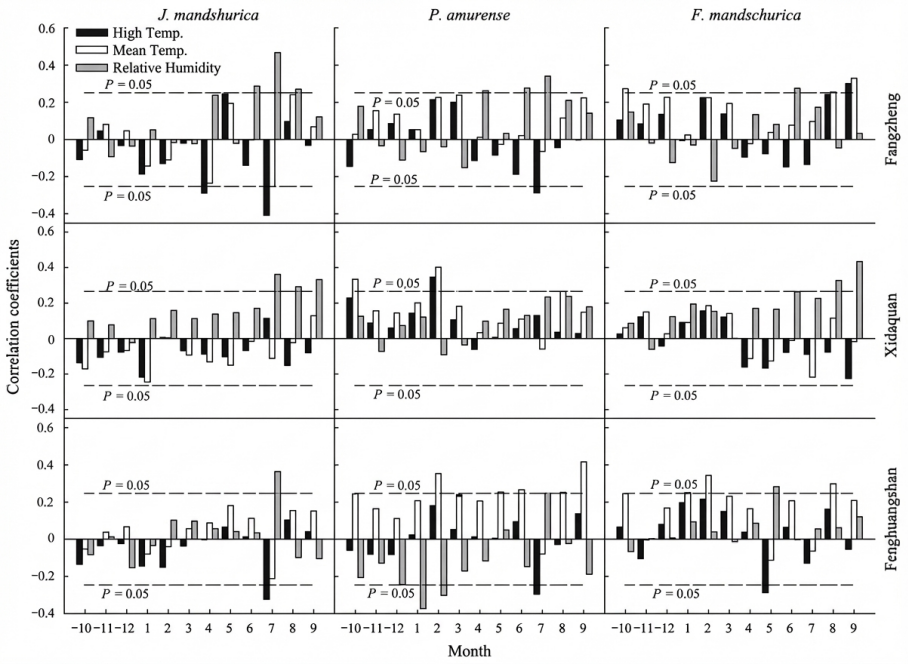

Figure 2: Figure 2

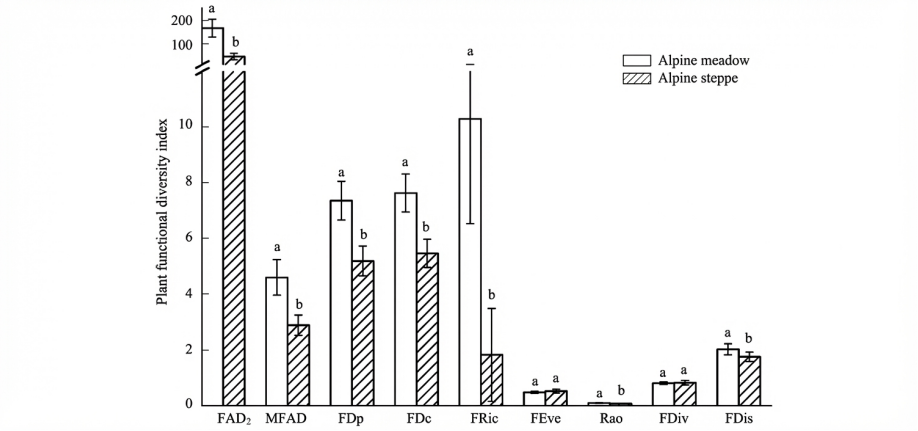

Figure 3: Figure 3

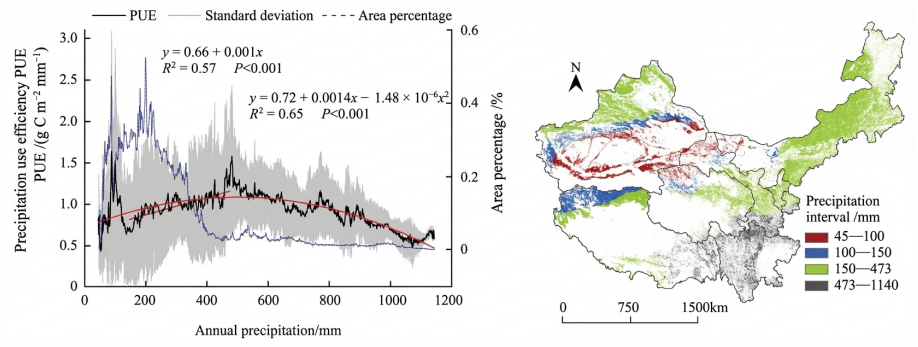

Figure 4: Figure 5

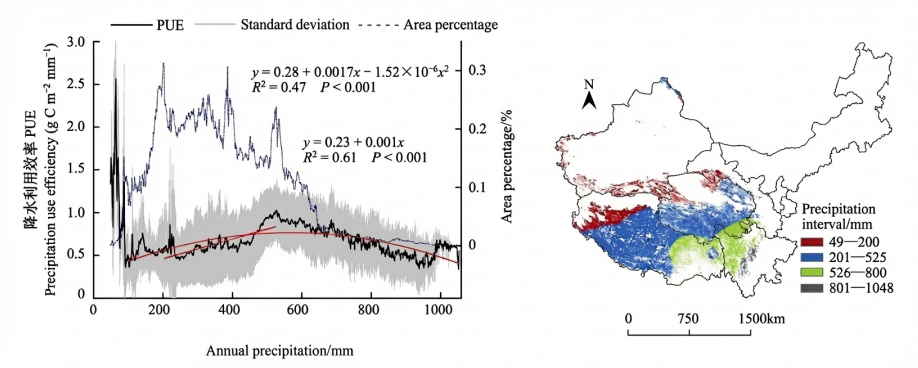

Figure 5: Figure 6

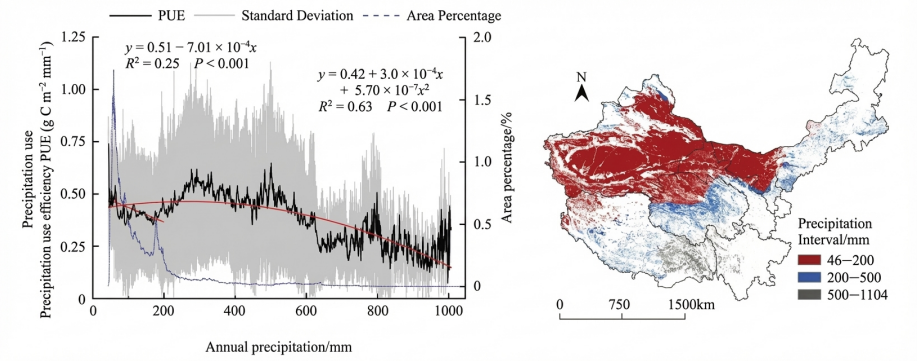

Figure 6: Figure 7

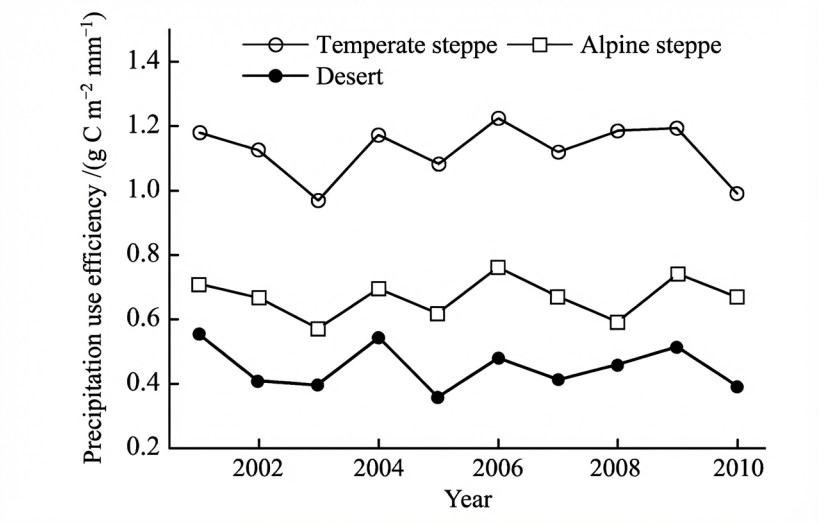

Figure 7: Figure 8

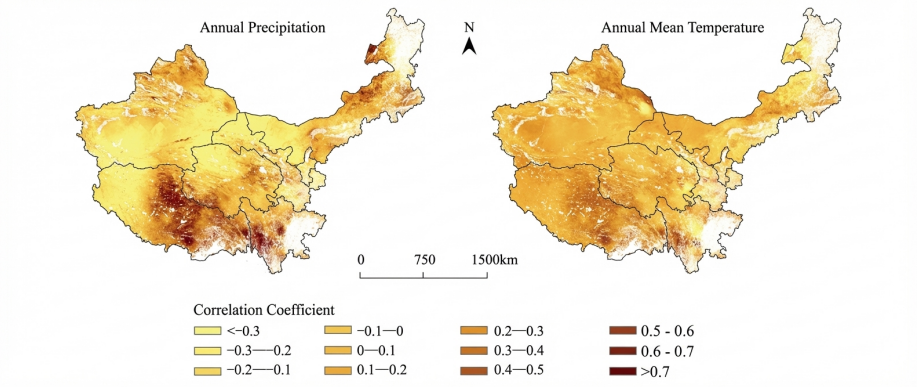

Figure 8: Figure 9

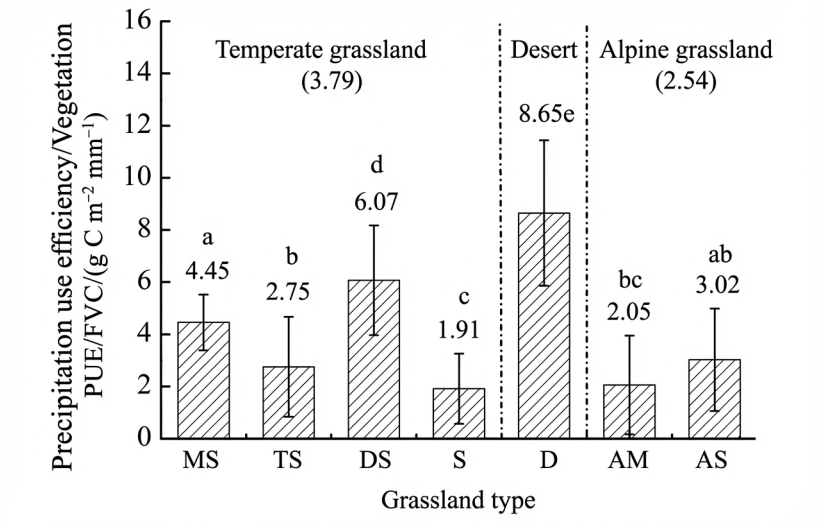

Figure 9: Figure 11

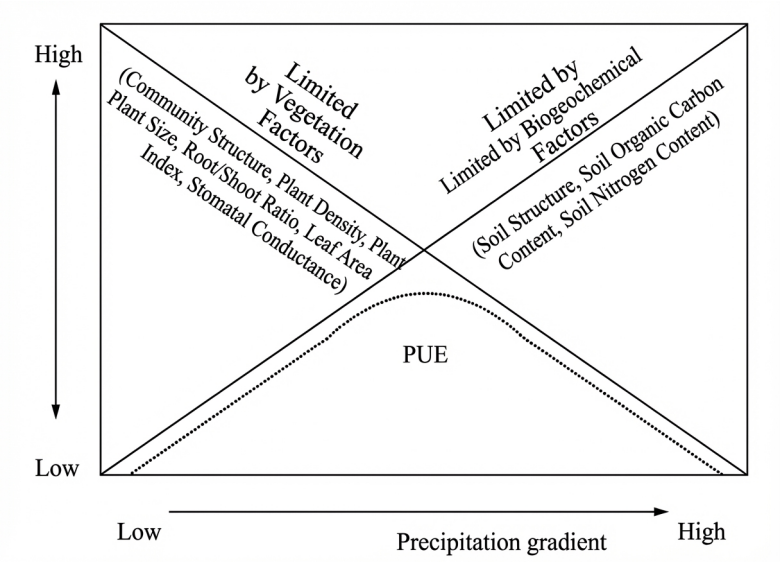

Figure 10: Figure 12

Figures

Source: ChinaXiv —Machine translation. Verify with original.